JOURNAL GEOLOGICAL SOCIETY OF INDIA
Vol.88, August 2016, pp.235-244

Comparison of Mineralization Pattern of Geochemical Data in Spatial and Position-scale Domain Using New DWT- PCA Approach

Hossein Shahi[1,2]*, Reza Ghavami[1] and Abolghasem Kamkar Rouhani[1]
[1]Faculty of Mining, Petroleum and Geophysics, Shahrood University, Shahrood, Iran
[2]Department of mining engineering, university of Gonabad, Gonabad, Iran
***Email**: hssn.shahi@gmail.com

Abstract: In the current research to determine the mineralization pattern and discuss the mineralization components, the information of position - scale domain of geochemical data has been analyzed. A new method is proposed based on coupling discrete wavelet transforms (DWT) and principal component analysis (PCA) for mineralization elements forecasting applications. The results of this study indicate the potential of DWT – PCA method for geochemical data processing. Wavelet transform (WT), as a multi-spectral analysis method, can decompose the spatial and temporal signals into different frequencies. The features of mineralization can be identified using the position - scale domain of geochemical data that may not be achievable in spatial domain. The geochemical data from the Dalli region have been processed in the spatial domain using PCA. The surface geochemical data of 30 elements have been transformed to position – scale domain using two-dimensional discrete wavelet transform (2DDWT). Wavelet functions (WFs) of Haar, Coiflet2, Biorthogonal3.3 and Symlet7 have been applied separately to decompose the geochemical data to high and low frequencies in one level. To obtain more accurate and complete information of mineralization, a new index has been presented based on wavelet coefficients. Based on this new index, significant results have been obtained by using PCA of the index. The coefficients distribution map (CDM) as a new exploratory criterion has been generated based on 2DDWT to show the geochemical distribution map (GDM). Finally, the results of WT have been compared with the results of spatial domain and the best method of wavelet for interpretation of geochemical data has been introduced. The results of geochemical data analysis by DWT – PCA approach have been confirmed by the exploratory drillings in the study area.

Keywords: Two dimensional discrete wavelet transform, Haar wavelet transform, Principal component analysis, Coefficients distribution map, Pattern recognition, Iran.

INTRODUCTION

Principal component analysis (PCA) is a multivariate statistical method for geo-information identification of geo-datasets (Cheng et al. 2011). The new space can typically be compressed into a few variables, which lets developers discard low variance variables and emphasize high-variance variables on the premise of minimizing data information loss. The covariance structure largely reflects the information (Zheng et al. 2006). In the PCA method, correlated variables with high dimensionality are transformed into several uncorrelated principal components, PCs, based on a covariance or correlation matrix (Loughlin 1991). To identify the mineralization factor(s) and determine the attributes of mineralization, PCA has been frequently used for analysis of geochemical data in spatial domain (Chandrjith et al. 2001; Cheng et al. 2006, 2011; Davis 2002; Garrett and Grunsky 2001; Reimann et al, 2002). Rao et al (2014) applied the PCA method on hydrogeochemical data for better understanding of the controlling processes that influence the aquifer chemistry. Yousefi et al (2012, 2014) applied the GMPI method based on factor scores values in PCA method to represent multi-element geochemical signature of the deposit-type sought on regional scale in spatial domain. Yousefi and Carranza (2015) improved the mineral prospectivity mapping using the fuzzification of continuous value spatial evidence in stream sediment samples. The geochemical interpretations have mostly been carried out in spatial domain. In addition to spatial domain, the frequency domain of geochemical data have been used to analyze the complex geochemical patterns (e.g., shahi et

al., 2014; Zou, 2011a,b; Hassani et al., 2009; Cheng and Zhao, 2011; Cheng et al., 2000; Afzal et al., 2012). Shahi et al (2014) applied PCA method on frequency domain of geochemical data to identify deep geochemical anomalies, sulfide zone and geochemical noises. In this paper, the position - scale domain of geochemical data, using 2DDWT, has been represented and analyzed for Cu–Au porphyry deposit in northern Dalli area and the results are discussed.

Wavelet analyses have led to very successful results in numerous scientific and engineering fields such as signal analysis and numerical applications (Li 1997; Zhang et al. 2003, 2006). A non-stationary signal can be decomposed into a number of stationary signals by wavelet analysis (Zhou et al. 2008). The multi-resolution analysis in wavelet analysis is a powerful tool for information analysis and processing that can extract information on various scales. The detailed information of spatial and frequency domains can be simultaneously analyzed with WT (Zhang et al. 2012). In the geochemical exploration research, wavelet analysis has been applied for processing oxygen isotope data in marine sediments (Bolton et al. 1995), noise reduction of the data in hydrocarbon geochemical exploration (Pei 1998), eliminating surface interference (Zhang et al. 2003; 2006) and fracture detection from water saturation log data (Tokhmechi et al. 2009). Wavelet analysis was also applied to eliminate to the influence of caprock thickness on anomaly intensities (Zhang et al. 2012).

GEOLOGY, ALTERATION AND MINERALIZATION OF THE STUDY AREA

Significant Cu porphyry deposits of Iran are related to calc–alkaline stocks in Sahand–Bazman, which is part of the Urmia–Dokhtar intrusive–volcanic belt (Hezarkhani 2006a, b; Hou et al. 2009). Dalli deposit is a part of this belt (Darabi-Golestan et al. 2013), which is located in the central province of Iran (Asadi Haroni 2008).

The mineralized Cu-Au zone in the study area is formed in the igneous diorite, quartz diorite porphyry, and volcanic rocks such as porphyritic amphibole andesite, andesite, dacite, and pyroclastics during the late Miocene to Pliocene (Fig. 1) (Asadi Haroni 2008). Based on the regional geology, the volcanic (porphyritic amphibole andesite, and dacite) and pyroclastics rocks in the study area are associated with late Miocene stratovolcanic rocks and are located in N-NE direction with a length of 30 km.

Mineralization in Northern Dalli occurs in granodiorite plutonic complex (tonalite), quartz diorite, and andesitic rocks. Potassic alteration occurred during the tonalitic intrusion and has included a larg amount of mineralization which includes quartz–potassium, feldspar–magnetite, and

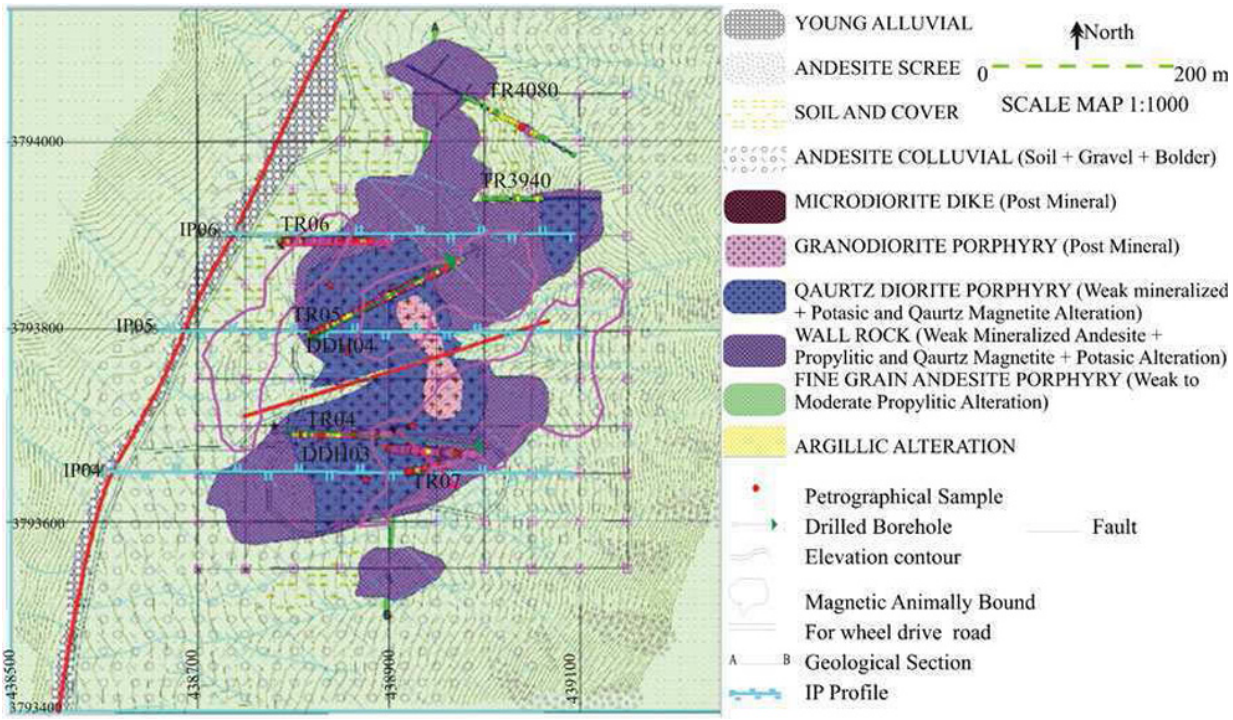

Fig.1. Local geological map of the Northern Dalli area showing the location of exploration survey (scale 1:1,000) (Darabi-Golestan et al. 2013; Asadi Haroni 2008)

biotite. The alteration zone in the study area covers an area of about 19.5 km^2. Potassic alteration is in the center of the area and is progressively surrounded by sericitic, sericite–chlorite and propylitic assemblages towards the border in porphyry deposits. In quartz diorite porphyry and andesite rocks, Cu–Au mineralization is related to potassic–phyllic and propylitic–silicic alteration, respectively (Darabi-Golestan et al. 2012). Magnetite is the predominant mineral in the potassic zone while sericite and chlorite minerals are less in this zone (Hezarkhani et al. 1999).

WAVELET TRANSFORM

WT is a tool for the analysis of de-noising and compression of signals (Grossman and Morlet 1984). Wavelets are used as the basis functions for signal and image representation such as sines and cosines in the Fourier transform (Morales and shih, 2000). Wavelet analysis is based on the similarity between the basic functions, wavelets, and frequency content of the signal (Nakhaei and Nasr 2012).

WT as a modern signal processing technique has shown better performance compared to Fourier transform (FT) and short time FT in analyzing non-stationary signals (Cartas et al. 2009). The FT will only provide the frequency information of a signal, while WT has the ability to simultaneously obtain information on the time, location and frequency of a signal (Partal 2009). Wavelet analysis is more flexible than Fourier analysis (Zhang et al. 2012). The continuous wavelet transform (CWT) of a signal x(t) is defined as (Partal 2009):

$$w(\tau,s)=\frac{1}{\sqrt{s}}\int_{-\infty}^{+\infty}x(t)\psi^{*}(\frac{t-\tau}{s})dt \qquad (\tau,s)\in R^2 \qquad (1)$$

where ψ is mother wavelet, t is the time, τ is the translation parameter, s is the wavelet scale and * denotes the conjugate complex function. The translation parameter τ is the time step in which the window function is iterated. w(τ, s) presents a two-dimensional picture of wavelet power under a different scale. Scaling either expands or compresses a signal (Cannas et al. 2006). The translation and dilation allow the WT to be localized in time and frequency (Graps 1995). The frequency has a reverse connection with the dilation parameter and compresses or stretches. The translation parameter determines the degree of window movement. The equation integration formula (1) should be resolved for different scales in the CWT. Calculating the wavelet coefficient is time consuming in all scales and produces a huge amount of data (Nakhaei and Naser, 2012). In DWT the scales and positions are selected based on powers of two, so called dyadic scales and positions. The signals are divided into approximation, which is high scale and low frequency components, that is low scale and high frequency components. After that the signal analysis is done quickly and precisely (Nakhaei and Nasr 2012). DWT is achieved by modifying the wavelet representation to (Grossman and Morlet 1984):

$$\psi_{m,n}(t)=s_0^{-m/2}\psi(\frac{t-n\tau_0 s_0^m}{s_0^m}) \qquad (2)$$

where s_0 is a specified fixed dilation step greater than 1, τ_0 is the location parameter that must be greater than zero, while m and n are integers that control, respectively, the scale and time. In the DWT, detailed and approximation coefficients are obtained with the wavelet algorithm based on high-pass and low-pass filters respectively (Zhang and Li, 2001). The filtering process is repeated every time and some frequencies in the signal are eliminated and the approximation of one or more details are obtained. (Adamowski and Chan, 2011). In this study, WFs of Haar, Coiflet2, Biorthogonal3.3 and Symlet7 were applied. These functions have been illustrated in Fig. 2.

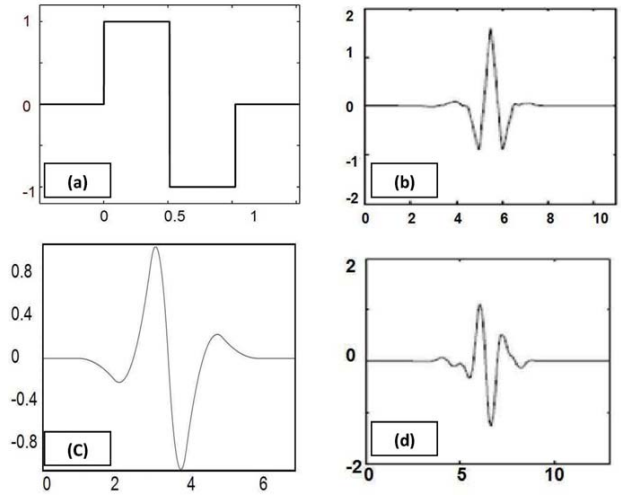

Fig.2. Wavelet functions of **(a)** Haar, **(b)** Coiflet 2, **(c)** Biorthogonal 3.3 and **(d)** Symlet 7 (Merry and Steinbuch, 2005).

DISCUSSION

Through systematic soil sampling, a grid net of 50×50 m^2 was sampled in Dalli area. 165 Samples with size fraction of "200 mesh were collected from the study area and were analyzed for 30 elements using inductively coupled plasma mass spectrometry (ICP-MS).

PCA method has been applied to the geochemical data in spatial domain. The PCA has divided the spatial domain data into 5 components (Table 1). Applications of the PCA method on spatial domain shows that the second principal

Table 1. Rotated component matrix in PCA method for spatial and position – scale domain (Haar wavelet function) of geochemical data

	Spatial domain data Component						Wavelet Transform(CL1 index) Component				
	1	**2**	3	4	5		**1**	2	3	4	5
Au	-0.193	**-0.631**	0.530	-0.430	0.049	**Au**	**-0.509**	-0.504	-0.408	-0.306	0.132
Al	0.792	0.325	-0.173	0.242	-0.151	Al	0.446	0.745	0.321	0.131	-0.107
As	-0.220	0.669	-0.074	0.336	-0.049	As	0.673	-0.189	0.234	0.147	-0.146
B	-0.024	0.776	-0.417	0.163	0.084	B	0.818	-0.003	0.077	0.374	-0.009
Ba	0.681	0.132	-0.212	0.090	0.379	Ba	0.088	0.646	0.059	0.289	0.339
Ca	0.199	0.326	-0.744	-0.212	-0.109	Ca	0.291	0.082	-0.265	0.800	-0.092
Ce	-0.186	0.205	0.105	-0.156	0.891	Ce	0.167	-0.105	-0.142	-0.003	0.923
Co	0.481	0.493	-0.035	0.298	-0.322	Co	0.547	0.399	0.349	0.077	-0.265
Cr	0.122	0.741	-0.128	-0.111	0.216	Cr	0.776	0.111	-0.094	0.222	0.175
Cu	-0.076	**-0.633**	0.473	-0.507	0.120	**Cu**	**-0.643**	-0.254	-0.497	-0.310	0.137
Fe	0.419	-0.167	0.729	-0.088	-0.069	Fe	-0.276	0.326	-0.200	-0.708	-0.109
Ga	0.848	0.035	0.130	0.067	-0.149	Ga	0.121	0.851	0.167	-0.182	-0.092
K	0.729	0.019	0.081	-0.366	0.210	K	0.053	0.766	-0.350	-0.138	0.121
La	-0.168	0.116	0.032	-0.126	0.899	La	0.094	-0.126	-0.151	0.050	0.914
Li	0.425	0.719	-0.371	0.102	0.211	Li	0.722	0.440	0.112	0.378	0.176
Mg	0.862	0.088	-0.168	-0.383	0.008	Mg	0.089	0.890	-0.322	0.156	0.020
Mn	0.323	0.835	0.134	0.080	0.006	Mn	0.881	0.235	0.012	-0.079	0.049
Mo	0.189	**-0.677**	0.313	0.208	0.217	**Mo**	**-0.563**	0.207	0.336	-0.006	0.163
Na	0.668	0.304	-0.047	0.398	-0.378	Na	0.249	0.601	0.415	-0.068	-0.478
Ni	0.027	0.896	-0.291	0.037	0.221	Ni	0.902	0.037	0.008	0.308	0.191
P	0.021	0.046	0.630	-0.177	0.109	P	0.019	0.027	-0.293	-0.598	-0.053
Pb	0.318	0.112	0.060	0.813	-0.172	Pb	0.167	0.222	0.829	0.000	-0.119
S	0.031	0.134	-0.403	0.741	-0.148	S	-0.086	-0.095	0.780	0.263	-0.172
Sc	0.839	-0.320	-0.133	0.090	0.117	Sc	-0.400	0.807	0.180	0.142	0.106
Sr	0.074	0.361	-0.728	0.335	-0.141	Sr	0.412	0.086	0.331	0.721	-0.197
Ti	0.498	-0.243	0.269	-0.712	0.088	Ti	-0.448	0.492	-0.636	-0.194	0.057
V	0.726	-0.187	0.426	0.034	-0.132	V	-0.228	0.719	0.005	-0.394	-0.220
Y	0.344	0.045	0.160	-0.087	0.796	Y	-0.039	0.454	-0.008	-0.124	0.770
Zn	0.664	0.336	0.242	0.240	-0.123	Zn	0.397	0.580	0.206	-0.242	-0.069
Zr	-0.044	0.778	0.161	0.251	0.175	Zr	0.827	-0.040	0.163	-0.088	0.237

component is related to the mineralization phase and contains the elements Au, As, B, Cr, Cu, Li, Mn, Ni, Mo and Zr. In this component Cu, Au and Mo have been separated with negative values. Factor two evaluates some other elements with positive values.

To determine the mineralization pattern and to discuss the mineralization components and identify the new exploration properties, spatial-domain geochemical data has been transferred to position – scale domain using 2DDWT. WFs of Haar, Coiflet2, Biorthogonal3.3 and Symlet7 have been applied separately to decompose the geochemical data to approximate and detail components in one level. Figure 3 illustrates the approximate and detail components of Cu in one level decomposition and reconstruction map of geochemical distribution using Haar discrete wavelet transform (HDWT). Detail component is calculated in the horizontal, vertical, and diagonal directions. Detail component represent high frequencies and large changes of concentration. Approximate component shows low frequencies and little changes of concentration and is similar to the initial geochemical distribution of elements. These maps present the wavelet coefficients with values from 0 to 250. The original map is the distribution map of elements in spatial domain that has been transferred to position – scale domain. The decomposition maps at level 1 as coefficient distribution maps (CDM) in position – scale domain have been calculated based on 2DDWT. These coefficients show the frequency distribution of elements in different scales and in vertical, horizontal and diagonal directions.

Wavelet coefficients demonstrate similarity between mother wavelet and geochemical distribution of elements on different scales. These coefficients have appropriate exploratory information that may be not achievable in spatial domain of geochemical data. These wavelet coefficients can be used for analysis of geochemical data. In this paper, a new method is proposed based on coupling DWT and PCA for mineralization elements forecasting applications. Therefore a new cumulative index, CL_1, is presented based on wavelet coefficients:

$$CL_1 = cA_1 + cd_{1h} + cd_{1v} + cd_{1d} \quad (3)$$

Where cd_{1d}, cd_{1h} and cd_{1v} are detail wavelet coefficients

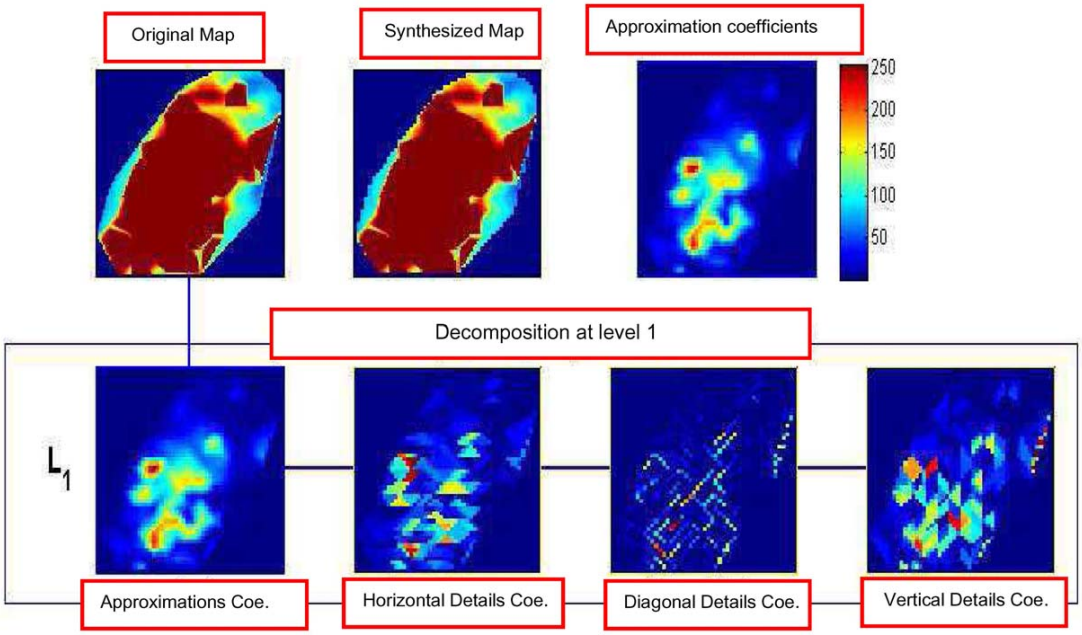

Fig.3. Schematic diagram of two-dimensional Cu geochemical distribution in one level of decomposition using Haar 2DDWT

matrix in diagonal, horizontal and vertical directions, respectively and cA_1 is approximate wavelet coefficients matrix in one level decomposition of elements. In fact, the similar values between the GDM and mother wavelet at different scales have been added together. Approximate and detail wavelet coefficients and subsequently index CL_1 correspond to variability in the concentration of elements so that the initial GDMs can be reconstructed using these coefficients. These wavelet coefficients contain the information of spatial and frequency domains simultaneously. Cumulative index CL_1 has been calculated for all 30 elements separately, and then, the PCA method has been applied on this index. The results of this analysis on the position – scale domain for Coiflet2, Biorthogonal3.3 and Symlet7 WFs are similar together (Tables 2 and 3). The PCA has divided these data into 6 components and third principal component has been recognized as mineralization factor. Application of the PCA method on position – scale domain (Coiflet 2 and Biorthogonal3.3 WFs) shows that the elements Au, Ca, Fe, Cu, P, S and Sr are related to the mineralization phase. The results of Symlet 7 WF shows that the elements Au, Ca, Fe, Cu, P, Pb, S, Ti and Sr exposure in the third principal component as mineralization phase.

The results of position – scale domain for Coiflet2, Biorthogonal3.3 and Symlet7 WFs has classified Mo element in factor 6.

PCA has classified the position – scale domain geochemical data (using Haar WF) into five components (Table 1). The number of principal components obtained in this analysis has been reduced in comparison to the components in Coiflet2, Biorthogonal3.3 and Symlet7 WFs. The first principal component, mineralization component consists of Au, Cu, Mo, As, B, Co, Cr, Li, Mn, Ni and Zr. Cu, Mo and Au have been classified in this factor with negative values. The results of this analysis on the position – scale domain (Haar WF) have identified the mineralizing elements of Au, Cu, Mo and also show the component of mineralization much better than the PCA results of the Coiflet2, Biorthogonal3.3 and Symlet7 WTs. Figure 4 illustrates the PCA values of mineralization factor in Coiflet2, Biorthogonal3.3, Symlet7 and Haar WTs.

The final analytical results of position – scale domain for these WFs and spatial domain of geochemical data have been given in Table 4.

The results obtained by new index CL_1 in Haar WF are same as the results of spatial domain. The Haar mother wavelet shows the results better than the other mother wavelets and is suitable for interpretation of geochemical data.

The results of applying PCA on the position – scale domain (HDWT) geochemical data have led to the determination of the Au, Cu and Mo elements as mineralizing factors. These results have been confirmed by borehole data and trenches in this study area. The results of chemical analyses show high concentrations of Au and Cu. An enrichment of Au and Cu in porphyry granodiorite stock illustrates a relationship with the contact of quartz diorite porphyry and andesite rocks. Figure 5 illustrates the PCA values of mineralization factor in spatial domain and HDWT (values in Table 1).

Table 2. Rotated component matrix in PCA method for position – scale domain (Bior 3.3 and Coiflet2 wavelet functions) of geochemical data

	Bior 3.3 Component							Coiflet 2 Component					
	1	2	**3**	4	5	6		1	2	**3**	4	5	6
Au	-0.45	-0.14	**-0.64**	-0.48	0.06	-0.01	**AU**	-0.42	-0.18	**-0.66**	-0.47	0.01	0.01
Al	0.32	0.64	0.24	0.54	-0.15	0.02	Al	0.31	0.62	0.29	0.57	-0.12	-0.02
As	0.60	-0.32	0.18	0.31	-0.01	0.11	As	0.64	-0.25	0.24	0.24	0.04	0.15
B	0.73	-0.07	0.38	0.18	0.01	0.30	B	0.77	-0.06	0.35	0.17	0.02	0.27
Ba	0.26	0.73	0.29	0.11	0.21	-0.13	Ba	0.25	0.75	0.29	0.16	0.17	-0.07
Ca	0.15	0.28	0.54	0.02	-0.02	0.68	Ca	0.17	0.28	0.53	0.06	-0.01	0.70
Ce	0.18	-0.08	-0.05	-0.13	0.94	0.02	Ce	0.16	-0.08	-0.04	-0.12	0.95	0.04
Co	0.31	0.23	0.14	0.67	-0.20	0.25	Co	0.36	0.28	0.17	0.67	-0.15	0.25
Cr	0.83	0.17	0.16	-0.04	0.06	0.05	Cr	0.82	0.17	0.23	0.00	0.02	0.02
Cu	-0.56	-0.16	**-0.51**	-0.43	0.18	0.16	Cu	-0.53	-0.19	**-0.53**	-0.42	0.15	0.15
Fe	-0.20	0.27	-0.80	0.18	-0.08	-0.05	Fe	-0.19	0.24	-0.80	0.26	-0.09	-0.02
Ga	0.08	0.77	-0.10	0.40	-0.15	-0.11	Ga	0.09	0.76	-0.03	0.44	-0.13	-0.18
K	0.10	0.85	-0.24	-0.05	0.03	0.02	K	0.08	0.86	-0.23	0.05	0.00	0.01
La	0.12	-0.09	0.00	-0.18	0.93	0.02	La	0.13	-0.10	-0.02	-0.18	0.93	0.04
Li	0.69	0.44	0.39	0.25	0.12	0.10	Li	0.66	0.44	0.45	0.27	0.11	0.08
Mg	0.03	0.93	-0.02	0.04	-0.03	0.28	Mg	0.02	0.93	0.03	0.11	-0.05	0.26
Mn	0.74	0.11	-0.08	0.45	0.07	0.32	Mn	0.74	0.05	0.02	0.50	0.04	0.27
Mo	-0.49	0.25	-0.04	0.02	0.06	**-0.59**	**Mo**	-0.54	0.25	0.00	0.06	0.03	**-0.55**
Na	0.16	0.46	0.10	0.58	-0.48	-0.12	Na	0.14	0.44	0.14	0.64	-0.43	-0.11
Ni	0.90	0.04	0.31	0.10	0.14	0.17	Ni	0.89	0.04	0.36	0.11	0.13	0.13
P	-0.06	-0.01	-0.67	-0.01	0.04	-0.05	P	-0.15	-0.02	-0.68	-0.01	0.04	-0.09
Pb	0.14	0.06	0.30	0.81	-0.07	-0.30	Pb	0.16	0.09	0.37	0.78	-0.03	-0.30
S	0.16	-0.08	0.63	0.49	-0.21	-0.19	S	0.20	-0.01	0.68	0.46	-0.16	-0.09
Sc	-0.31	0.80	0.20	0.28	0.06	-0.11	Sc	-0.37	0.81	0.17	0.23	0.07	-0.05
Sr	0.25	0.03	0.76	0.36	-0.09	0.31	Sr	0.29	0.08	0.74	0.33	-0.05	0.39
Ti	-0.42	0.60	-0.44	-0.28	0.07	0.31	Ti	-0.43	0.59	-0.48	-0.22	0.02	0.32
V	-0.20	0.63	-0.40	0.39	-0.22	-0.07	V	-0.20	0.59	-0.37	0.50	-0.21	-0.02
Y	-0.01	0.46	-0.10	0.13	0.73	-0.18	Y	-0.05	0.47	-0.03	0.17	0.72	-0.22
Zn	0.23	0.38	-0.18	0.75	0.05	0.24	Zn	0.25	0.34	-0.12	0.79	0.05	0.20
Zr	0.87	-0.05	-0.01	0.14	0.15	-0.23	Zr	0.86	-0.01	0.04	0.15	0.18	-0.29

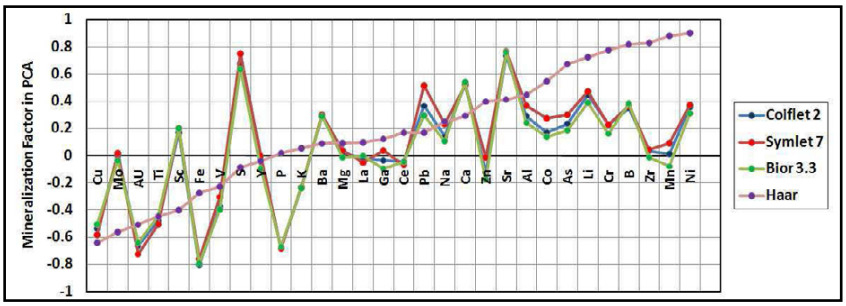

Fig.4. PCA values of mineralization factors in position – scale domain (Coiflet 2, Symlet 7, Bior 3.3 and Haar WFs)

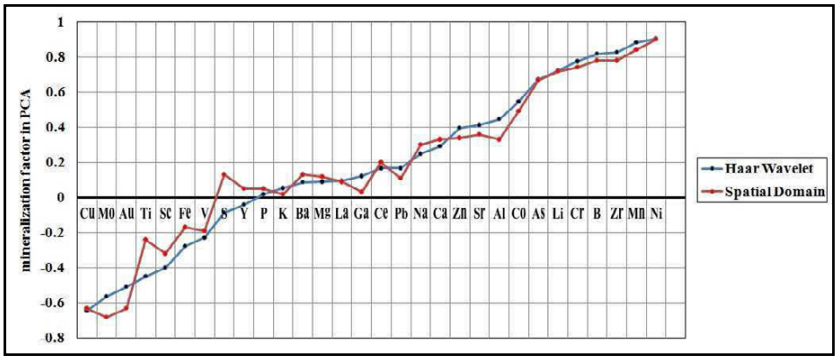

Fig.5. PCA values of mineralization factors in spatial and position – scale domain (Haar WT)

Table 3. Rotated component matrix in PCA method for position – scale domain (Symlet 7 wavelet function) of geochemical data

	Symlet 7 Component					
	1	2	**3**	4	5	6
Au	-0.43	-0.22	**-0.72**	-0.35	0.00	0.04
Al	0.31	0.64	0.37	0.51	-0.12	-0.05
As	0.64	-0.25	0.30	0.22	0.10	0.16
B	0.76	-0.06	0.37	0.16	0.03	0.28
Ba	0.27	0.75	0.30	0.11	0.15	-0.05
Ca	0.14	0.28	0.52	0.07	-0.01	0.71
Ce	0.16	-0.08	-0.07	-0.09	0.96	0.04
Co	0.33	0.30	0.27	0.66	-0.14	0.20
Cr	0.82	0.14	0.23	-0.02	0.00	0.07
Cu	-0.54	-0.22	**-0.58**	-0.31	0.15	0.17
Fe	-0.19	0.23	-0.76	0.38	-0.10	-0.04
Ga	0.10	0.78	0.04	0.40	-0.13	-0.20
K	0.08	0.85	-0.23	0.07	0.00	0.02
La	0.13	-0.11	-0.05	-0.14	0.93	0.05
Li	0.66	0.45	0.48	0.21	0.09	0.11
Mg	0.00	0.93	0.04	0.11	-0.05	0.26
Mn	0.72	0.05	0.09	0.54	0.03	0.25
Mo	-0.48	0.26	0.02	0.00	0.00	**-0.59**
Na	0.15	0.47	0.23	0.58	-0.43	-0.15
Ni	0.88	0.04	0.37	0.08	0.11	0.17
P	-0.16	-0.01	-0.68	0.03	0.06	-0.15
Pb	0.14	0.08	0.52	0.67	0.00	-0.35
S	0.23	0.03	0.75	0.33	-0.16	-0.09
Sc	-0.35	0.82	0.20	0.18	0.06	-0.08
Sr	0.28	0.10	0.77	0.26	-0.05	0.38
Ti	-0.46	0.57	-0.51	-0.13	0.02	0.33
V	-0.19	0.60	-0.30	0.54	-0.23	-0.06
Y	-0.03	0.49	0.00	0.15	0.71	-0.25
Zn	0.24	0.35	-0.01	0.82	0.04	0.14
Zr	0.87	0.01	0.05	0.11	0.17	-0.26

In this diagram, the scores of elements in mineralization factor have been illustrated for HWT and spatial domain. Cu, Au and Mo have successfully been separated from other elements using CL_1 index in Haar WT. Therefore new index CL_1 in Haar WT can be especially useful for analysis of geochemical data.

GDM in spatial domain based on the results of PCA has been depicted (Fig.6b). Factor 2 as a mineralization factor in PCA consists of Cu, Au, and Mo. Factor scores for all samples have been delineated to show GDM. The trenches, IP profiles, drilled boreholes and the direction of these boreholes have also been shown in the figure. The results of position – scale domain have high diversity and given more exploratory information than spatial domain. CL_1 index as a new exploratory criterion in position – scale domain has been analyzed using PCA method (Table 1). Factor1 as a mineralization factor consists of Cu, Au, and Mo. The scores of all samples in this factor that related to Haar wavelet transform coefficients have been depicted to create the coefficient distribution map (CDM). The CDM in position – scale domain can desirably show the GDM in spatial domain (Fig.6a). The obtained results from drilled boreholes and trenches confirm the results of CDM in Haar WT. The diagonal details of coefficients in decomposition of level 1 show the high geochemical frequencies that related to high diametrical variability of the elements. The CDM of cd_{1d} can desirably shows the high diametrical variability in GDM and is related to the mineralization trend. Hence, the boreholes and trenches can be designed based on CDM of cd_{1d}. The CDM of cd_{1d} for Cu element has been calculated and depicted in Fig.6c. The IP profiles, boreholes and trenches have been illustrated in the CDM of cd_{1d}. The CDM of cd_{1d} for Cu element shows the mineralization trend that has mostly been located in NE direction. In the study area, the volcanic and pyroclastics rocks are also located in N-NE direction based on the regional geology. The drilled boreholes and trenches show the mineralization intensity as well as the results of CDMs of cd_{1d} and CL_1 index.

Information obtained from the exploration drillings in the study area confirm the analytical results of Haar WT of geochemical data. Borehole DDH03 has been drilled in the study area (Figs. 1 and 6). There are supergene, transition and hypogen zones in the study area. The type of ore minerals defines the boundary of these zones. In the study area, potassic alteration associates with chalcopyrite, bornite, and/or minor molybdenite intergrowth with quartz. Distribution of Cu-Au and Mo elements in borehole DDH03 is shown in Figs. 7 and 8, respectively. There is a clear trend in variations of Cu, Au, and Mo in the study area. There is a sequential enrichment of Mo→Cu→Au from the intrusive rock (granodiorite rock) to the contact of quartz diorite porphyry, andesite and wall rock in the mineralized zone.

CONCLUSIONS

In this study, in order to determine the mineralization

Table 4. The final results of position – scale domain for Coiflet2, Biorthogonal3.3 and Symlet7 WFs and spatial domain of geochemical data

	Spatial domain	Haar WF	Biorthogonal3.3 WF	Coiflet2 WF	Symlet7 WF
Mineralization component	Negative values: (Au, Cu, Mo)	Negative values: (Au, Cu, Mo)	Negative values (Au, Fe, Cu, P)	Negative values: (Au, Fe, Cu, P)	Negative values: (Au, Fe, Cu, P, Ti)
	Positive values : (As, B, Cr, Li, Mn, Ni, Zr)	Positive values : (As, B, Co, Cr, Li, Mn, Ni, Zr)	Positive values: (S, Sr, Ca)	Positive values: (S, Sr, Ca)	Positive values: (S, Sr, Ca, Pb)

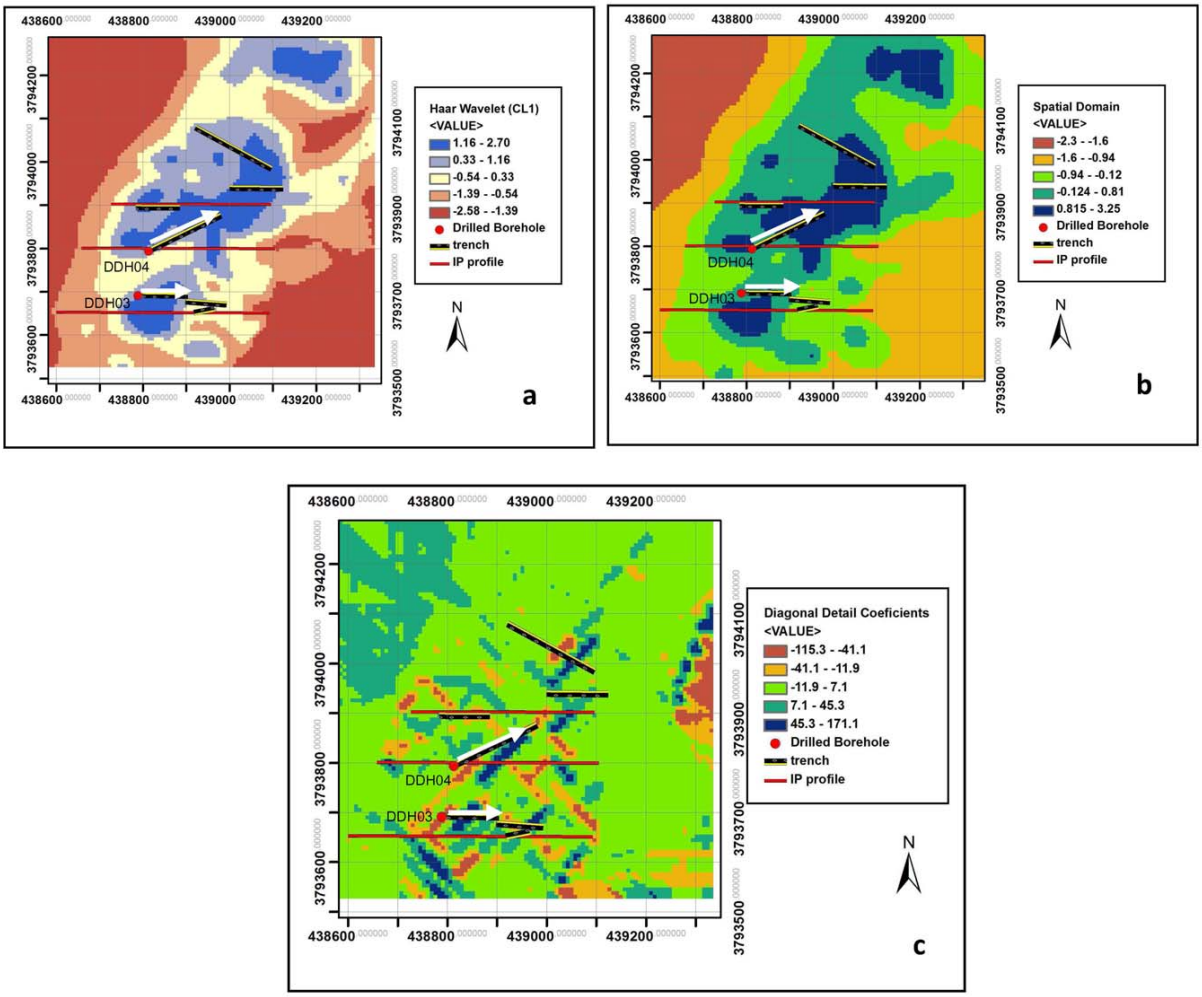

Fig.6. Geochemical distribution maps, a: Map of interpolated scores of mineralization factor in position - scale domain using Haar WT (CDM of F1 in CL_1 index), b: Map of interpolated scores of mineralization factor in spatial domain (F2), c: CDM of diagonal detail in first level of decomposition for Cu element using Haar WT

pattern and identify the elements related to mineralizing phase, the PCA method has been applied on spatial and position – scale domains of soil geochemical data in Dalli area. 2DDWT, which can capture the multi-scale features of signals, has successfully been used to decompose the geochemical distribution of elements and transfer them to position – scale domain. The wavelet coefficients of geochemical data have appropriate exploratory information that may be not achievable in the spatial domain. Therefore a new cumulative index, CL_1, has been presented based on

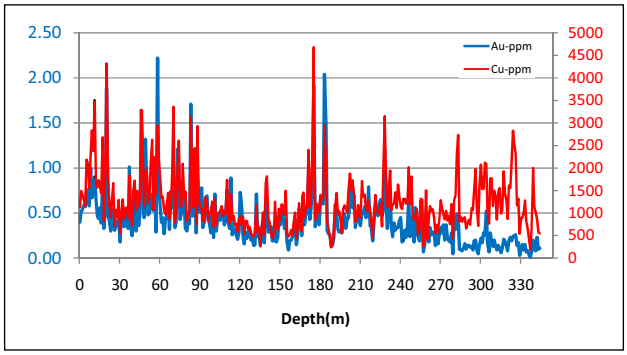

Fig.7. Variations of Cu versus Au in borehole DDH03

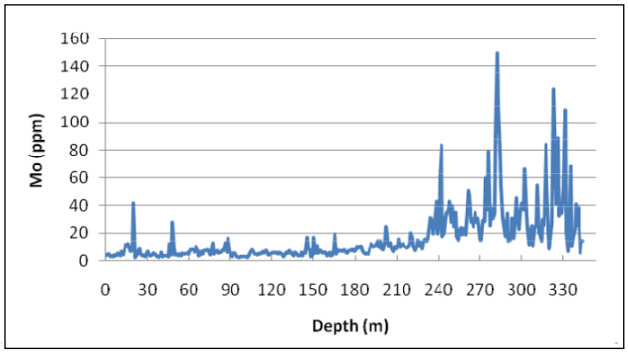

Fig.8. Variations of Mo values in borehole DDH03

wavelet coefficients, and PCA has been performed on this index. The results of this analysis on the position – scale domain for Coiflet2, Biorthogonal3.3 and Symlet7 WFs are together similar. The results of this analysis on the Haar WT have desirably identified the mineralizing elements of Au, Cu, Mo and also have shown the component of mineralization much better than the PCA results of the other WFs. Hence, the Haar wavelet is a suitable mother wavelet for interpretation of geochemical data. The two CDMs based on CL_1 index and cd_{1d} can illustrate the GDM and the variability of mineralization. The CDM obtained from 2DDWT, a newly proposed approach, has high ability for facilitating analysis of geochemical data and designing the trenches, boreholes and geophysical profiles. Information obtained from the exploration drillings in the study area confirms the analytical results of WT of geochemical data. The results of this study indicate the potential of DWT – PCA models as pattern recognition and useful for interpretation of geochemical data.

References

Adamowski, J. and Chan, H.F. (2011) A wavelet neural network conjunction model for groundwater level forecasting. Jour. Hydrol., v.407(1), pp.28-40.

Asadi Haroni, H. (2008) First Stage Drilling Report on Dalli Porphyry Cu-Au Prospect, Central Province of Iran. Technical Report.

Afzal, P., Fadakar Alghalandis, Y., Moarefvand, P., Rashidnejad Omran, N. and Asadi Haroni, H. (2012) Application of power-spectrum–volume fractal method for detecting hypogene, supergene enrichment, leached and barren zones in Kahang Cu porphyry deposit,Central Iran, Jour. Geochem. Explor., v.112, pp.131-138.

Bolton, E.W, Maasch, K.A. and Lilly, J.M. (1995) A wavelet analysis of Plio-Pleistocene climate indicators: A new view of periodicity evolution. Geophys. Res. Lett., v.22(20), pp.2753-2756.

Cannas, B., Fanni, A., See, L. and Sias, G. (2006) Data preprocessing for river flow forecasting using neural networks: wavelet transforms and data partitioning. Physis and Chemistry of the Earth, v.31(18), pp.1164-1171.

Cartas, R., Moreno-Barón, L., Merkoçi, A., Alegret, S., del Valle, M., Gutiérrez, J.M., Leija, L., Hernandez, P.R. and Muñoz, R. (2009) Multivariate calibration model for a voltammetric electronic tongue based on a multiple output wavelet neural network. Biologically Inspired Signal Processing, SCI, v.188, pp.137-167.

Chandrajith, R., Dissanayake, C.B. and Tobschall, H.J. (2001) Application of multi-element relationships in stream sediments to mineral exploration: a case study of Walawe Ganga Basin, Sri Lanka. Applied Geochem., v.16(3), pp.339–350.

Cheng, Q., Xu, Y. and Grunsky, E. (2000). Integrated Spatial and Spectrum Method for Geochemical Anomaly Separation. Natural Resources Research, v.9, No.1.

Cheng, Q., Jing, L. and Panahi, A. (2006) Principal component analysis with optimum order sample correlation coefficient for image enhancement. Internat. Jour. Remote Sensing, v.27 (16), pp.3387-3401.

Cheng, Q., Bonham-Carter, G., Wang, W., Zhang, S., Li, W. and Xia, Q. (2011) A spatially weighted principal component analysis for multi-element geochemical data for mapping locations of felsic intrusions in the Gejiu mineral district of Yunnan, China. Computers & Geosciences, v.37, pp.662-669.

Cheng, Q. and Zhao, P. (2011) Singularity theories and methods for characterizing mineralization processes and mapping geo-anomalies for mineral deposit prediction. Geoscience Frontiers, v.2(1), pp.67-79.

Darabi-Golestan, F., Ghavami-Riabi R. and Asadi-Harooni, H. (2013) Alteration, zoning model, and mineralogical structure considering lithogeochemical investigation in Northern Dalli Cu–Au porphyry. Arabian Jour. Geosci., v.6(12), pp.4821-4831.

Davis, J.C. (2002) Statistics and Data Analysis in Geology, John Wiley and Sons, New York. 638p.

Garrett, R.G. and Grunsky E.C. (2001) Weighted sums—knowledge based empirical indices for use in exploration geochemistry. Geochemistry: Exploration Environment Analysis, v.1, pp.135-141.

Graps, A. (1995) An introduction to wavelets. Computational Science & Engineering, IEEE, v.2(2), pp.50-61.

Grossmann, A. and Morlet, J. (1984) Decomposition of Hardy functions into square integrable wavelets of constant shape. SIAM Jour. Mathematical Analysis, v.15(4), pp.723-736.

Hassani, H., Daya, A. and Alinia, F. (2009) Application of a fractal method relating power spectrum and area for separation of geochemical anomalies from background. Aust. Jour. Basic Appld. Sci., v.3(4), pp.3307-3320.

Hezarkhani, A. (2006a) Hydrothermal evolution of the Sar-Cheshmeh porphyry Cu–Mo deposit. Iran: evidence from fluid inclusions. Jour. Asian Earth Sci., v.28, pp.409-422.

Hezarkhani, A. (2006b) Petrology of the intrusive rocks within the Sungun porphyry copper deposit, Azerbaijan, Iran. Jour. Asian Earth Sci., v.27, pp.326-340.

Hezarkhani, A., Williams-Jones, A.E. and Gammons, C.H. (1999) Factors controlling copper solubility and chalcopyrite deposition in the Sungun porphyry copper deposit, Iran. Mineralium Deposita, v.34(8), pp.770-783.

Hou, Z., Yang, Z., Qu, X., Meng, X., Li, Z., Beaudoin, G. and Zaw, K. (2009) The Miocene Gangdese porphyry copper belt generated during post-collisional extension in the Tibetan Orogen. Ore Geol. Rev., v.36(1), pp.25-51.

Li, J. (1997) Wavelet analysis and signal processing—theory,

application and software. Chongqing Publishing House, Chongqing, pp.1–325 (in Chinese)

Loughlin, W.P. (1991) Principal component analysis for alteration mapping. Photogrammetric Engineering and Remote Sensing, v.57(9), pp.1163-1169.

Merry, R.J.E. and Steinbuch, M. (2005) Wavelet theory and applications. A literature study, Eindhoven University of Technology.

Morales, E. and Shih, F.Y. (2000) Wavelet coefficients clustering using morphological operations and pruned quadtrees. Pattern Recognition, v.33(10), pp.1611-1620.

Nakhaei, M. and Nasr, A.S. (2012) A combined Wavelet-Artificial Neural Network model and its application to the prediction of groundwater level fluctuations. Geopersia, v.2(2), pp.77-91.

Partal, T. (2009) River flow forecasting using different artificial neural network algorithms and wavelet transform. Canadian Jour. Civil Engg., v.36(1), pp.26-38.

Pei, T. (1998) Spatial structure analysis of geochemical field of oil and gas and its application to exploration in North Tarim Basin: PhD thesis No. Bo 9817, China University of Geosciences, Wuhan, P. R. China, pp.1–65 (in Chinese).

Rao, N.S., Vidyasagar, G., Rao, P.S. and Bhanumurthy, P. (2014) Assessment of hydrogeochemical processes in a coastal region: application of multivariate statistical model. Jour. Geol. Soc. India, v.84(4), pp.494-500.

Reimann, C., Filzmoser, P. and Garrett, R.G. (2002) Factor analysis applied to regional geochemical data: problems and possibilities. Appld. Geochem, v.17(3), pp.185-206.

Shahi, H., Ghavami, R., Kamkar Rouhani, K. and Asadi-Haroni, H. (2014). Identification of mineralization features and deep geochemical anomalies using a new FT-PCA approach, Jour. Geopersia, v.4(2), pp.101-110.

Tokhmechi, B., Memarian, H., Rasouli, V., Noubari, H. A. and Moshiri, B. (2009) Fracture detection from water saturation log data using a Fourier–wavelet approach. Jour. Petrol. Sci. Engg., v.69(1), pp.129-138.

Yousefi, M., Kamkar-Rouhani, A. and Carranza, E.J.M. (2012) Geochemical mineralization probability index (GMPI): a new approach to generate enhanced stream sediment geochemical evidential map for increasing probability of success in mineral potential mapping. Jour. Geochem. Explor., v.115, pp.24-35.

Yousefi, M., Kamkar-Rouhani, A. and Carranza, E.J.M. (2014) Application of staged factor analysis and logistic function to create a fuzzy stream sediment geochemical evidence layer for mineral prospectivity mapping. Geochemistry: Exploration, Environment, Analysis, v.14(1), pp.45-58.

Yousefi, M. and Carranza, E.J.M. (2015) Fuzzification of continuous-value spatial evidence for mineral prospectivity mapping. Computers & Geosciences,v.74, pp.97-109.

Zeng, A., Pan, D., Zheng Q.L. and Peng, H. (2006) Knowledge acquisition based on rough set theory and principal component analysis. Intelligent Systems, IEEE, v.21(2), pp.78-85.

Zhang, X. and Li, D. (2001) A Trous decomposition applied to image edge detection. Geographic Information Science v.7(2), pp.119-123.

Zhang, L., Bai G. and Xu, Y. (2003) A wavelet-analysis-based new approach for interference elimination in geochemical hydrocarbon exploration. Mathematical Geol., v.35(8), pp.939-952.

Zhang, L., Bai, G., Zhao, K. and Sun, C. (2006) Restudy of acid-extractable hydrocarbon data from surface geochemical survey in the Yimeng Uplift of the Ordos Basin, China: improvement of geochemical prospecting for hydrocarbons. Marine and Petroleum Geol., v.23(5), pp.529-542.

Zhang, L., Bai, G. and Zhao, Y. (2012) A method for eliminating caprock thickness influence on anomaly intensities in geochemical surface survey for hydrocarbons. Mathematical Geosciences, v.44(8), pp.929-944.

Zhou, H.C., Peng, Y. and Liang, G.H. (2008) The research of monthly discharge predictor-corrector model based on wavelet decomposition. Water Resources Management, v.22, pp.217-227.

Zuo, R. (2011a) Identifying geochemical anomalies associated with Cu and Pb–Zn skarn ineralization using principal component analysis and spectrum–area fractal the Gangdese Belt, Tibet (China). Jour. Geochem. Explor., v.111, pp.13-22.

Zuo, R. (2011b) Decomposing of mixed pattern of arsenic using fractal model in Gangdese belt, Tibet, China. Applied Geochem., v.26, pp.S271-S273.

(Received: 7 September 2014; Revised form accepted: 16 July 2015)